PLANT signaling & behavior

Plant Signaling & Behavior

ISSN: (Print) (Online) Journal homepage: https://www.tandfonline.com/loi/kpsb20

PRC2-mediated H3K27me3 modulates shoot iron homeostasis in *Arabidopsis thaliana*

Emily Y. Park , Kaitlyn M. Tsuyuki , Elizabeth M. Parsons & Jeeyon Jeong

To cite this article: Emily Y. Park , Kaitlyn M. Tsuyuki , Elizabeth M. Parsons & Jeeyon Jeong (2020): PRC2-mediated H3K27me3 modulates shoot iron homeostasis in *Arabidopsis thaliana* , Plant Signaling & Behavior, DOI: 10.1080/15592324.2020.1784549

To link to this article: https://doi.org/10.1080/15592324.2020.1784549

Published online: 27 Jun 2020.

PLANT SIGNALING & BEHAVIOR
https://doi.org/10.1080/15592324.2020.1784549

Taylor & Francis
Taylor & Francis Group

RESEARCH PAPER

PRC2-mediated H3K27me3 modulates shoot iron homeostasis in *Arabidopsis thaliana*

Emily Y. Park, Kaitlyn M. Tsuyuki, Elizabeth M. Parsons, and Jeeyon Jeong

Department of Biology, Amherst College, Amherst, MA, USA

ABSTRACT

Plants use intricate mechanisms to adapt to changing iron conditions because iron is essential and also one of the most limiting nutrients for plant growth. Furthermore, iron is potentially toxic in excess and must be tightly regulated. Previously, we showed that chromatin remodeling via histone 3 lysine 27 trimethylation (H3K27me3) modulates the expression of FIT-dependent genes under iron deficiency in roots. This study builds on our previous findings, showing that H3K27me3 also modulates iron regulation in shoots. In the *clf* mutant, which lacks the predominant H3K27 tri-methyltransferase, we detected increased iron translocation to shoots under iron deficiency as compared to wild type. Transcriptomic analysis of shoots also revealed differential expression of genes consistent with higher iron levels in *clf* shoots than wild type shoots under iron-deficient conditions. In addition, we verify that *YSL1* and *IMA1*, two genes involved in signaling iron status from shoots to roots, are direct targets of H3K27me3 and reveal iron-dependent deposition of H3K27me3 on these loci. This study contributes to a better understanding of the molecular mechanisms behind iron regulation in plants, as the effect of PRC2-mediated H3K27me3 on iron homeostasis genes expressed in the shoots has not been previously reported to our knowledge.

ARTICLE HISTORY
Received 12 May 2020
Revised 12 June 2020
Accepted 14 June 2020

KEYWORDS
Iron; shoot; homeostasis; H3K27me3; CLF; transcriptome; Arabidopsis

Introduction

As photosynthetic organisms, plants have a unique need for iron because iron is used as an essential cofactor for chlorophyll biosynthesis and photosynthesis, in addition to playing essential roles in metabolic processes conserved across photosynthetic and non-photosynthetic organisms. However, iron is one of the most limiting nutrients for plant growth. At the same time, plants must prevent or counteract cytotoxic reactive oxygen species (ROS) that can be generated by dysregulated iron homeostasis. Therefore, plants have evolved elaborate strategies to tightly regulate iron. Understanding the molecular mechanisms of iron homeostasis in plants is of high significance for agriculture and human health, as it will provide us with the knowledge to help improve plant growth and enhance the content of bioavailable iron in crops.

Upon iron deficiency, a large number of genes involved in iron acquisition and translocation are induced in plants. This so-called iron-deficiency response is elaborately regulated at the transcriptional through post-translational levels.[1-4] In Arabidopsis, at least 16 basic-helix-loop-helix (bHLH) transcription factors are involved in transcriptional regulation of the iron-deficiency response.[3] FER-LIKE IRON DEFICIENCY-INDUCED TRANSCRIPTION FACTOR (FIT) positively regulates iron-acquisition genes via interacting with the bHLH subgroup Ib transcription factors bHLH38, bHLH39, bHLH100, or bHLH101 to induce Strategy I iron-acquisition genes.[5-9] Strategy I is a reduction-based mechanism dicotyledonous plants use to uptake iron, which involves the efflux of protons by *P*-type H^+-ATPases[10] and coumarins by PDR9,[11,12] reduction of ferric-chelates to ferrous iron by FERRIC REDUCTASE OXIDASE 2 (FRO2),[13] and transport of ferrous iron into the root epidermal cell by Iron-Regulated Transporter 1 (IRT1).[14-17]IRT1 can directly sense excess metals to regulate its own degradation.[18] FIT has been considered to be the master regulator of Strategy I, but remains subjected to complex iron-dependent regulation at the transcriptional and post-translational levels.[5,19-21] Recently, Upstream Regulator of IRT1 (URI)/bHLH121 has been identified as a positive regulator that acts upstream of FIT.[22,23] *URI/bHLH12* is ubiquitously expressed in various tissues regardless of iron conditions but is phosphorylated under iron deficiency and induces *bHLH38/39/100/101*, which encode transcription factors that heterodimerize with FIT.[22,23]

POPEYE (PYE), another bHLH protein, is induced in the pericycle and negatively regulates genes involved in iron mobilization and translocation.[24] Some of its targets include *NICOTIANAMINE SYNTHASE 4 (NAS4)*, which encodes an enzyme that synthesizes nicotianamine (NA) that chelates iron for vascular translocation, [25] and *FRO3*, which encodes a mitochondrial ferric-chelate reductase expressed in the vasculature.[26] *PYE* is tightly co-regulated with *BRUTUS (BTS)*, which encodes a RING E3 ligase with hemerythrin/HHE iron-binding domains.[24] BTS is stable under low iron and negatively regulates group IVc transcription factors that interact with PYE.[27] Two BTS paralogs, BTS-LIKE 1 (BTSL1) and BTSL2, have also been shown to negatively regulate the iron-deficiency response.[28] BTS regulates the abundance of bHLH104 and bHLH105[27] as well as phosphorylated URI upon iron re-supply.[22] The heterodimer of URI/bHLH121 and IAA-LEUCINE RESISTANT 3 (ILR3), or its close homologs, directly regulates multiple iron homeostasis genes, such as

CONTACT Jeeyon Jeong jjeong@amherst.edu Department of Biology Amherst College, Amherst, MA, USA

BTS, PYE, and *bHLH38/39/100/101*, and indirectly controls *FIT*.[22,23]

Iron acquired by the roots is translocated to the shoots through the xylem as an iron-citrate complex; Ferroportin 1/Iron-Regulated Protein 1 (FPN1/IREG1) effluxes iron from the pericycle to the xylem, [29] where iron forms a complex with citrate and is released to the apoplastic space by FERRIC REDUCTASE DEFECTIVE 3 (FRD3).[30] Apoplastic iron ions are transported into the phloem by Oligo Peptide Transporter 3 (OPT3) for long-distance transport.[31] NA is a non-proteinogenic amino acid that binds to iron and other transition metals.[32] Iron-NA complexes move laterally from the vasculature to neighboring parenchymal cells via Yellow Stripe-Like (YSL) family transporters such as YSL1, YSL2, and YSL3.[33-35]

In the leaves, iron is required for chlorophyll biosynthesis and is in high demand in the photosynthetic electron transport chain. To maintain appropriate iron levels while preventing iron-induced oxidative stress, plants must be able to coordinately respond to the needs in the leaves and the availability of iron in the rest of the plant. Iron sensing and signaling mechanisms are not as well understood as iron acquisition. However, multiple studies have provided evidence that, in addition to local signals in the roots, long-distance signals generated based on the shoot iron status control iron uptake in the roots.[36-41] Notably, many molecular players of iron translocation in Arabidopsis are critical in long-distance iron signaling. For example, the *ysl1ysl3* double mutant is unable to induce iron-deficiency response in the roots, [42] whereas *opt3-2, frd3/man1*, and the quadruple nicotianamine synthase mutant *nas4x-1* constitutively express iron-acquisition genes.[31,43,44] Small peptides of the IRON MAN (IMA) or FE-UPTAKE-INDUCING PEPTIDE (FEP) family have also been proposed to signal iron from shoots to roots. These peptides are highly expressed in the phloem and positively regulate the iron-deficiency response.[45,46]

Our recent work established that Histone 3 lysine 27 trimethylation (H3K27me3) contributes to the regulation of the FIT-dependent iron-deficiency response through direct targeting of *FIT, FRO2*, and *IRT1*.[47] H3K27me3 is a widespread repressive epigenetic modification, which is regulated by polycomb-group protein complexes and is critical in gene regulation and multicellular development.[48,49] In Arabidopsis, H3K27me3 is established by polycomb repressive complex 2 (PRC2), which contains the methyltransferase subunits CURLY LEAF (CLF) and SWINGER (SWN). CLF and SWN are partially redundant, but CLF predominantly accounts for the H3K27 trimethyltransferase activity of PRC2.[50,51] There is a strong correlation between the sites of PRC2 binding and H3K27me3 deposition in Arabidopsis, [52] unlike in Drosophila where spreading of H3K27me3 can occur far beyond PRC2 binding sites.[53] Using the *clf* mutants, in which PRC2-mediated H3K27me3 deposition is significantly reduced, we identified that the loci of *FIT, FRO2*, and *IRT1* are H3K27me3-enriched under iron-sufficient conditions. However, once exposed to iron-deficient conditions, H3K27me3 is partially removed to allow the induction of these FIT-dependent genes. Additionally, in *clf* mutants, the induction of *FIT* and its target genes was pronouncedly higher than in wild type. Based on these observations, we proposed that PRC2-mediated H3K27me3 attenuates the induction of iron-acquisition genes in the roots to protect against iron toxicity.

In this study, we build on our prior work by investigating the response to iron deficiency in *clf* shoot tissue. To our knowledge, the role of H3K27me3 on iron homeostasis in shoots has not been reported. We provide evidence that iron homeostasis genes highly expressed in the shoots, such as *YSL1* and *IMA1*, are direct targets of PRC2-mediated H3K27me3. Our results suggest that H3K27me3 contributes to regulating iron homeostasis genes in the shoots by modulating iron translocation from roots to shoots.

Materials and methods

Plant materials and growth conditions

Arabidopsis plants were grown at 22°C under a 16/8 h light/dark cycle. For the treatment in Figure 1(a), plants were germinated and grown on iron-deficient media (-Fe) of Murashige and Skoog (MS) medium with no iron (Caisson MSP33) supplemented with 300 μM ferrozine or iron-sufficient media (+Fe) of MS medium with 100 μM FeNa-EDTA (Caisson MSP34) for up to 12 d. The concentration of 100 μM iron is comparable to that of multiple classical plant media formulations such as Gamborg's B5 and MS basal salts.[54,55] For the iron deficiency treatment in Figure 2(a), plants were germinated and grown on Gamborg's B5 medium without sucrose for up to 12 d, then transferred to -Fe or +Fe media and grown for 3 d. The *Arabidopsis thaliana* ecotype Columbia (Col-0) was used as the wild type, and the *clf* mutant used was *clf-29* (SALK_21003) obtained from the Arabidopsis Biological Resource Center.

ICP-MS analysis

Iron content of wild type and *clf* roots and shoots was measured by ICP-MS. Plants were grown as indicated, and dried tissue was weighed in a microbalance and digested with nitric acid. Elemental content was analyzed with the Perkin-Elmer NexION 350D ICP-MS at the Mass Spectrometry Core, Institute for Applied Life Science at University of Massachusetts, Amherst. Metal content was normalized to the dry mass (mg) of each sample.

RNA extraction

Total RNA was isolated from roots and shoots using the Plant RNA Isolation Kit (Agilent) following the manufacturer's instructions. The quantity and purity of RNA were assessed using NanoDrop One (Thermo Scientific), and the integrity of RNA was examined by electrophoresis in a bleach gel.[56]

RNA-sequencing and data analysis

RNA was extracted from three biological replicates of wild type and *clf* shoots treated under iron deficient or sufficient conditions for 3 d as described above. cDNA library construction, 150 bp paired-end sequencing on Illumina NovaSeq6000 platform, and standard RNA-seq analysis were conducted by

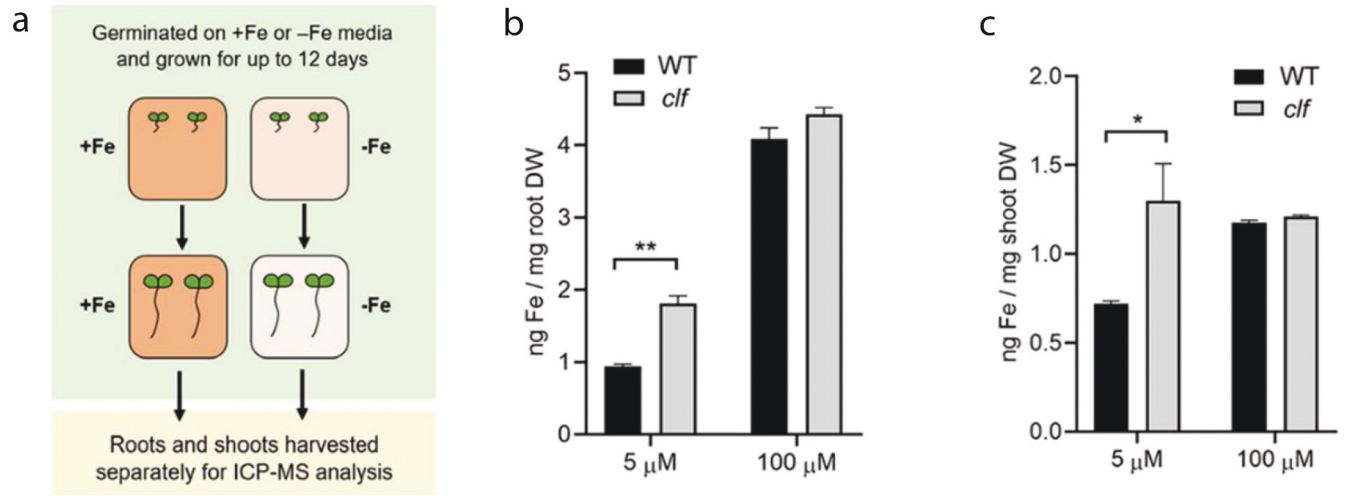

Figure 1. Iron content of *clf* and wild type plants germinated in low iron or iron-sufficient conditions. (a) Schematic overview of the sample growth conditions (b) Iron content of root tissue from plants germinated and grown in media with 5 µM Fe (low iron) or 100 µM Fe (sufficient iron). (c) Iron content of shoot tissue from the same plants analyzed in (B). Mean values of five pooled samples are shown with error bars (SE). Significant differences compared to wild type based on t-tests are denoted (*: $p < .05$; **: $p < .01$).

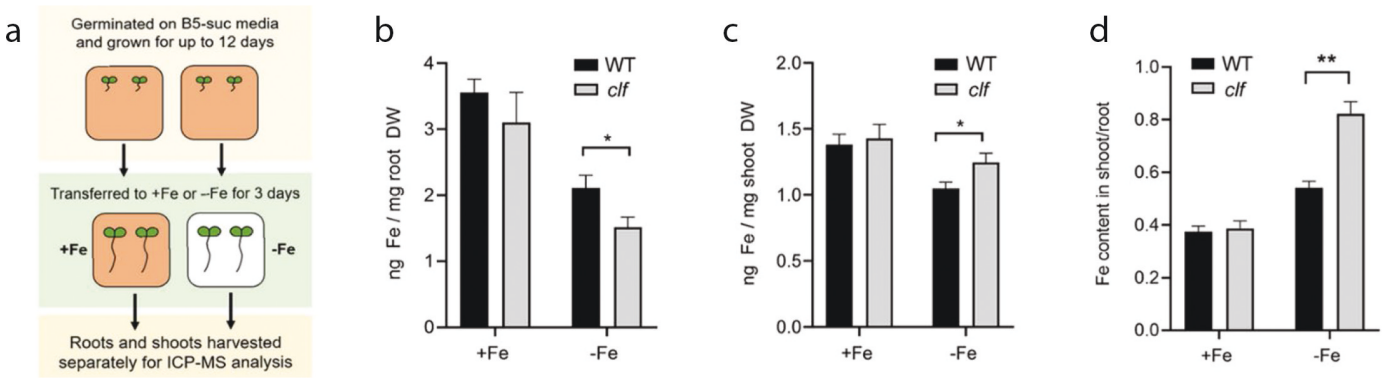

Figure 2. Iron content of *clf* and wild type plants treated in iron-deficient or sufficient media for 3 d. (a) Schematic overview of the sample growth conditions (b) Iron content of roots from 12-d-old plants grown on B5 without sucrose and then transferred to iron sufficient (+Fe; 100 µM Fe) or iron-deficient (-Fe; 300 µM ferrozine) media for 3 d. (c) Iron content of shoots from the same batch of plants analyzed in (B). (d) Relative level of iron translocation as measure by the ratio of iron content in shoots versus roots. Mean values of five pooled samples are shown with error bars (SE). Significant differences compared to wild type based on t-tests are denoted (*: $p < .05$; **: $p < .01$).

Novogene. Gene expression was quantified using the union mode of the HTSeq software and reported as FPKM (Fragments Per Kilobase of transcript sequence per Millions of base pairs sequenced). Sequencing reads were aligned to the TAIR10 *Arabidopsis thaliana* reference genome (www.arabidopsis.org), and Integrative Genomics Viewer (IGV), IGV 2.4[57,58] was used to generate read count histograms. Differential gene expression analysis was performed with DESeq (padj < 0.05) using negative binomial distribution for *p*-value estimation and BH for FDR estimation.[59] The enrichment analysis tool[60] available from the Gene Ontology Consortium[61,62] was used for Gene Ontology (GO) term enrichment analysis.

ChIP-qPCR

ChIP was conducted with shoot tissues of wild type and *clf* plants following the procedure described.[47] Briefly, shoot tissue was infiltrated with 37% formaldehyde in GB buffer (0.4 M sucrose, 10 mM Tris pH 8.0, 1 mM EDTA) and 100 mM PMSF to crosslink proteins with gDNA, ground in liquid nitrogen, and then sonicated in lysis buffer (500 mM HEPES pH 7.5, 150 mM NaCl, 1 mM EDTA, 1% Triton X-100, 0.1% deoxycholate, 0.1% SDS) using Bioruptor Pico (Diagenode). Crosslinked DNA was precleared with Protein A Agarose/Salmon Sperm DNA beads (Millipore Sigma, 16–157) for 1 h at 4°C with gentle rotation and then incubated with anti-IgG (Millipore Sigma 12–370), anti-H3 (AbCam1791), or anti-H3K27me3 antibodies (Millipore Sigma07-449) overnight at 4°C with gentle rotation. After washing with a series of lysis buffer, LNDET buffer (0.25 M LiCl, 1% NP-40, 1% deoxycholate, 1 mM EDTA, 10 mM Tris-HCl pH 8.0), and TE buffer, the crosslinked DNA was eluted with elution buffer (1% SDS, 0.1 M $NaHCO_3$). Proteinase K was used to reverse crosslinking, and chromatin DNA was purified using the Zymo-Spin ChIP Kit per manufacturer's instructions. qPCR was conducted using Power SYBR Green PCR Master Mix (Applied Biosystems) in QuantStudio 3 Real-Time PCR System

(Applied Biosystems), and gene enrichment was normalized to 10% of input.[63] Primers were designed using QuantPrime.[64] The primer sequences used for qPCR are *IMA1/FEP* forward: 5′-GGCCATCAAGAGATTTGACCATGC- 3′; *IMA1/FEP3* reverse: 5′-TGCCACTCGAGAACTATCTACCAC-3′; *YSL1* forward: 5′-CTGCGGTTCTC-ATCAATGGCTTCC-3′; *YSL1* reverse: 5′-GAAACCACGCACTTGTTTCCTGCAAATC-3′.

Results

Iron content is higher in roots and shoots of *clf* than in wild type germinated and grown in low iron

Our previous study showed that *clf* loss-of-function mutants expressed higher levels of FIT-regulated genes involved in iron acquisition, such as *FIT, IRT1, FRO2*, and *F6′H1*, and exhibited better growth with longer roots under prolonged iron deficiency, i.e., when plants were germinated and grown in low iron conditions compared to wild type plants.[47] Despite the partial redundancy between CLF and SWN, we did not use the *clf swn* double mutant for our experiments due to its severe phenotypes and development into a mass of callus-like tissue without distinct roots or shoots.[50] The *clf* mutant used in this study, *clf-29*, is a well-established H3K27me3 mutant with a remarkably reduced level of H3K27me3 and has been used in multiple studies, [65–70] including our previous report.[47] To follow up with the low iron growth phenotype and to test if iron uptake was enhanced in *clf* plants, we used inductively coupled plasma mass spectrometry (ICP-MS) to quantify iron content in roots and shoots of wild type and *clf* seedlings germinated in media with low iron (5 μM Fe) or sufficient levels of iron (100 μM Fe), the same conditions for germination and growth tests with *clf* mutants in our prior study.[47] Iron content was significantly higher in both roots and shoots of *clf* plants germinated and grown in low iron media (Figure 1(b,c)), which is consistent with both the enhanced induction of iron uptake genes and better growth in *clf* under iron-deficient conditions as previously reported.[47] As predicted, the iron content of *clf* roots or shoots was not significantly different from that of wild type plants when germinated and grown in iron-sufficient media (Figure 1(b,c)).

Iron translocation from roots to shoots is enhanced in *clf* after iron-deficiency treatment

To examine iron content and translocation in *clf* plants upon transition into iron deficiency, we germinated wild type and *clf* plants in iron-sufficient medium and then treated in iron sufficient or deficient media for 3 d (Figure 2(a)). This 3-d iron treatment was long enough to induce the expression of iron-acquisition genes without causing visible growth phenotypes in *clf* plants.[47] We predicted that iron uptake and thus iron content in roots would be greater in *clf* plants than in wild type due to enhanced expression of FIT-dependent iron-acquisition genes in *clf*. Unexpectedly, under iron-deficient conditions, the iron content of *clf* roots was lower than that of wild type roots (Figure 2(b)); however, *clf* shoot tissue contained 19% more iron than wild type shoots (Figure 2(c)). The relative amount of iron translocated from roots to shoots, as determined by the ratio of shoot to root iron content, was approximately 50% higher in *clf* plants treated under iron-deficient conditions than in wild type (Figure 2(d)). This increased iron translocation in *clf* suggests that *clf* plants might still be transporting more iron into their roots, as we predicted, but not accumulating iron in their roots. Furthermore, these results imply a differential response to iron deficiency in *clf* shoot tissues.

Transcriptomic analysis of genes differentially regulated by iron in *clf* and wild type shoots

To examine the effect of H3K27me3 on transcriptional regulation in shoots under iron deficiency and to find clues to explain the increased translocation of iron to shoot tissue detected in *clf* plants (Figure 2(d)), we performed RNA-seq analysis with the wild type and *clf* shoot tissue from plants treated in iron deficient and sufficient media for 3 d, i.e., the same growth conditions represented in Figure 2(a), which were used in our previous transcriptomic analyses with root samples.[47]

We conducted hierarchical clustering with 1628 genes differentially expressed in wild type or *clf* shoots (Figure 3). A large proportion of shoot genes exhibited a genotype-specific expression pattern (Figure 3), contrary to the expression profile in the roots where differentially regulated genes primarily responded to iron regardless of the genotype.[47] However, we identified 621 and 270 genes differentially regulated by iron in wild type shoots and in *clf* shoots, respectively, and noted four groups of iron-regulated genes based on the cluster analysis (Figure 3).

Group I

The first group of interest consisted of genes that accumulated less mRNA transcript under iron-sufficient conditions than in

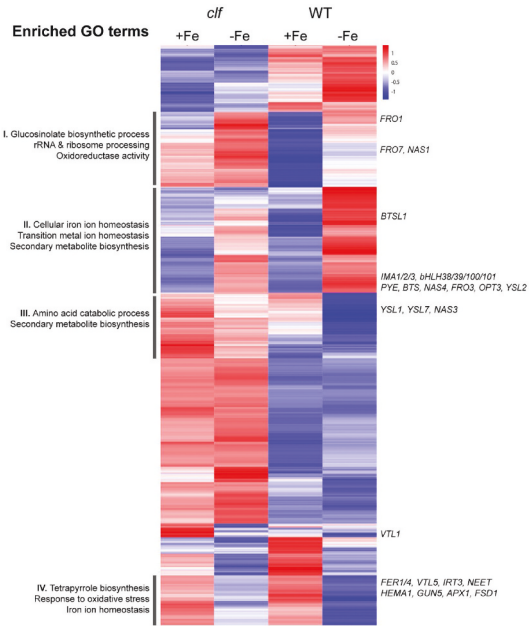

Figure 3. Cluster analysis of genes differentially regulated by iron in wild type and *clf* shoots. Heat map of genes differentially regulated by iron in wild type or *clf* shoot tissue. Enriched GO terms and known iron homeostasis genes are indicated. Numbers on the scale bar represent standard deviation from the mean.

iron-deficient conditions in both genotypes, but had higher steady-state mRNA level in *clf* than in wild type regardless of the iron conditions (Figure 3). Genes involved with glucosinolate biosynthesis were enriched in this region. Glucosinolates are sulfur-rich compounds that are integral to plant defense mechanisms, [71] and iron serves as a cofactor of specifier proteins involved in glucosinolate breakdown.[72] However, the implications of differential expression of glucosinolate biosynthetic genes remain to be understood. Ribosomal RNA and ribosome processing genes were also overrepresented in this group. Pan et al. (2015) found post-transcriptionally induced changes in ribosomal protein composition in iron deficiency and proposed that the ribosomes might be specialized in iron-deficient conditions. In their study, the abundance of a large number of ribosomal proteins was pronouncedly increased, but significant changes at the transcriptional level had not been detected.[73] Further studies will be necessary to determine if the detected transcriptional response in ribosomal genes under iron-deficient conditions in *clf* (Figure 3) is consistent with the post-transcriptional changes in ribosomes reported by Pan et al. (2015). Another enriched GO term from this group was oxidoreductase activity, and *FRO1* and *FRO7*, which encode ferric-chelate reductases that belong to the family of oxidoreductases, were found in this category. FRO7 is involved in chloroplast iron acquisition,[74] but the role of FRO1 remains to be understood.

Group II

The second category was comprised of genes that had a higher steady-state mRNA level under iron deficiency in wild type shoots but were not as responsive to iron deficiency in the *clf* mutant (Figure 3). Group II was overrepresented with iron or transition metal homeostasis genes and genes involved in secondary metabolite biosynthesis. Multiple known iron homeostasis genes induced by iron deficiency, such as *IMA1/2/3, bHLH38/39/100/101, BTS, BTSL1, PYE, NAS3/4, FRO3, OPT3*, and *YSL2* were found in this group (Figure 3). Many of these genes are highly expressed in the vasculature.[75] Under iron-sufficient conditions, the Group II genes accumulated more mRNA in *clf* or had similar mRNA levels in both genotypes (Figure 3). Since H3K27me3 serves as a repression mark, the reduced mRNA level of Group II genes in *clf* under iron-deficient conditions is more likely due to higher iron content in *clf* shoots compared to wild type (Figure 2) instead of a direct effect of PRC2-mediated regulation.

Group III

Genes with less mRNA accumulation under iron deficiency in wild type but not in *clf*, and genes with a higher level of mRNA under iron-sufficient conditions in *clf* than in wild type shoots were found in the third group (Figure 3). Given the higher mRNA accumulation level in *clf* under, both iron conditions, the genes identified in this group are more likely to be under H3K27me3-mediated control than genes associated with the other groups. The enriched GO terms in this category were amino acid catabolic processes and secondary metabolite biosynthesis. Iron homeostasis genes that play critical roles in iron translocation were also identified in this group. For example, *NAS3*, which encodes an enzyme in the biosynthetic pathway of NA, a non-proteinogenic amino acid, [76] and *YSL1* and *YSL7*, which encode transporters of iron-NA complexes, [77] were found in this region.

Group IV

This category consisted of genes that had increased mRNA accumulation under iron sufficiency and reduced mRNA accumulation under iron limiting conditions in both wild type and *clf*, but whose differences in steady-state mRNA level were not as robust in *clf* compared to wild type (Figure 3). Genes involved in tetrapyrrole or heme biosynthesis and photosynthesis were highly enriched in this region (Figure 3). Considering the essential role of iron in these processes, the differential mRNA accumulation of genes in this group is consistent with the greater iron levels in *clf* shoots than in wild type under iron deficiency (Figure 2). Genes that play roles in oxidative stress response and iron homeostasis were also overrepresented in this category including *FER1* and *FER4*, which encode ferritins that sequester iron to prevent iron-induced oxidative stress, [78] *VTL5*, which is positively regulated by iron supply and encodes a vacuolar iron importer that can buffer cytosolic iron, [79] and *APX1* and *FSD1*, which encode enzymes that detoxify reactive oxygen species.[80,81] The enhanced expression of genes that buffer iron and mitigate oxidative stress in Group IV is consistent with the higher iron content in *clf* shoots under iron-deficient conditions (Figure 3).

H3K27me3 deposition levels on *YSL1* are consistent with the iron-dependent expression of *YSL1*

YSL1 is expressed in the shoots, but its expression is decreased under iron deficiency.[82] Consistently, in both wild type and *clf* mutant, *YSL1* transcript level was higher in shoot tissue from plants treated in iron-sufficient media compared to those treated in iron-deficient media (Figure 4(a); Table 1). However, we detected markedly enhanced expression of *YSL1* in *clf* compared to wild type, *YSL1* expression in *clf* shoots was increased ~2.5-fold under iron-sufficient conditions and increased ~6-fold under iron-deficient conditions (Figure 4(a); Table 1). The higher expression of *YSL1* in *clf* than in wild type is in accordance with the more robust iron translocation from roots to shoots in *clf* plants as determined by our ICP-MS analysis (Figure 2).

Based on the significant increase in *YSL1* expression in *clf* shoots regardless of the iron conditions (Figure 4(a); Table 1), we predicted that H3K27me3 deposition might be associated with the repression of *YSL1* in iron deficiency. To our knowledge, the *YSL1* locus was identified as an H3K27me3 target in at least one epigenetic study[83] but was not among the H3K27me3 direct targets identified in multiple other studies that detected other iron homeostasis genes.[84-88] Furthermore, whether or not H3K27me3 deposition on *YSL1* depends on iron condition had not been studied. Our ChIP-qPCR showed that H3K27me3 accumulated at the *YSL1* locus in wild type shoots under iron deficiency (Figure 4(b)), verifying that *YSL1* is a direct target of H3K27me3, and revealed a strong correlation between H3K27me3 levels and *YSL1* repression in wild type and *clf* shoots (Figure 4). Furthermore, our data revealed about 2-fold enrichment of H3K27me3 in wild type shoots

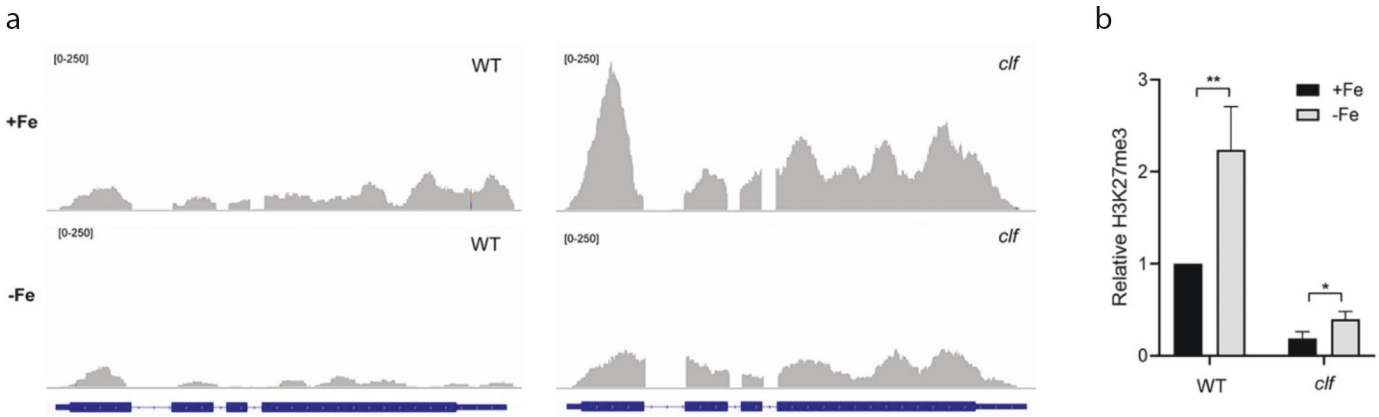

Figure 4. ***YSL1*** **transcript level and H3K27me3 deposition in wild type and** ***clf*** **shoots**. (a) RNA-seq read count histograms of *YSL1* in wild type and *clf* shoots under iron deficient and sufficient conditions. Gene diagrams depict introns (line) and exons (boxes) and are aligned with read counts. The read count range is denoted in the upper left corner of each diagram. Read count scale is equivalent for wild type and *clf* within each gene. (b) H3K27me3 deposition at *YSL1* locus. ChIP-qPCR signal was normalized with input DNA, and H3K27me3 enrichment relative to that of wild type grown under iron-sufficient conditions was plotted. Error bars represent standard error of the mean of four biological replicates and significant differences compared to wild type based on t-tests are denoted (n = 4; *: $p < .05$).

Table 1. Relative expression (log_2 fold change) of select iron-regulated genes expressed in wild type and *clf* shoots.

Gene ID	Gene Name	Annotated Function	WT -Fe vs. WT +Fe	*clf* -Fe vs. *clf* +Fe
At1g01590	*Ferric Reductase Oxidase 1 (FRO1)*	reduces ferric-chelate iron to ferrous iron	4.91	1.68
At1g09240	*Nicotianamine Synthase 3 (NAS3)*	synthesizes nicotianamine	−3.21	−1.24
At1g21140	*Vacuolar Iron Transporter-Like 1 (VTL1)*	catalyzes Fe transport into the vacuole	−4.11	−1.60
At1g23020	*Ferric Reductase Oxidase 3 (FRO3)*	reduces ferric-chelate iron to ferrous iron	4.54	3.86
At1g47400	*Fe-Uptake Inducing Peptide 3/Ironman 1 (FEP3/IMA1)*	regulator of the iron deficiency response	10.60	8.65
At1g58290	*HEMA1*	protoporphyn biosynthesis	−3.73	−2.27
At2g30766	*Fe-Uptake Inducing Peptide 1/Ironman 3 (FEP1/IMA3)*	regulator of the iron deficiency response	6.31	5.29
At2g38460	*Ferroportin 1/Iron Regulated 1 (FPN1/IREG1)*	transmembrane iron transporter	−0.36	−0.15
At2g40300	*Ferritin 4 (FER4)*	sequesters iron in mitochondria and plastids	−3.17	−1.91
At2g41240	*bHLH100*	heterodimerizes with FIT to activate iron deficiency response	13.05	9.68
At3g18290	*Brutus (BTS)*	negative regulator of the iron deficiency response	3.79	3.19
At3g25190	*Vacuolar Iron Transporter-Like 5 (VTL5)*	catalyzes Fe transport into the vacuole	−4.53	−4.01
At3g56090	*Ferritin 3 (FER3)*	sequesters iron	−1.87	0.21
At3g56970	*bHLH038*	heterodimerizes with FIT to activate iron deficiency response	11.48	10.14
At3g56980	*bHLH039*	heterodimerizes with FIT to activate iron deficiency response	10.01	8.92
At4g16370	*Oligopeptide transporter 3 (OPT3)*	phloem iron transporter	3.63	2.68
At4g24120	*Yellow Stripe Like 1 (YSL1)*	iron-nicotianamine transmembrane transporter	−2.41	−1.11
At4g25100	*Fe-Superoxide Dismutase 1 (FSD1)*	dismutates superoxide during oxidative stress	−2.47	−1.09
At5g01600	*Ferritin 1 (FER1)*	sequesters iron in plastids	−3.91	−2.04
At5g04150	*bHLH101*	heterodimerizes with FIT to activate iron deficiency response	7.46	7.15
At5g04950	*Nicotianamine Synthase 1 (NAS1)*	synthesizes nicotianamine	1.54	0.59
At5g24380	*Yellow Stripe-Like 2 (YSL2)*	iron-nicotianamine transmembrane transporter	1.57	0.96
At5g51720	*NEET*	2Fe-2 S cluster binding	−5.30	−3.50

from plants treated in iron-deficient media than in iron-sufficient media, which was consistent with the significant repression of *YSL1* under iron deficiency (Figure 4; Table 1). While H3K27me3 deposition was low in *clf* shoots under both iron conditions, there was a clear correlation between H3K27me3 levels and the extent of *YSL1* repression. The H3K27me3 levels in iron-sufficient *clf* shoots were only about half (~48%) of that in iron-deficient *clf* shoots, inversely correlating with the relative level of *YSL1* under the two conditions (Figure 4; Table 1). These results suggest the involvement of H3K27me3 in iron-dependent regulation of *YSL1* expression.

IMA1 is a direct target of PRC2-mediated H3K27me3

IMA1 transcripts accumulated under iron deficiency in both wild type and *clf* shoots, consistent with previous studies,[45,46] but the induction of *IMA1* in *clf* shoots was less than that in wild type shoots; the fold change induced by iron deficiency in *clf* and wild type was 402 and 1548, respectively (Figure 5(a); Table 1). We noted that the *IMA1/FEP3* locus was identified as an H3K27me3 target in multiple large-scale epigenomic datasets (Table 2).[8,85-88] To examine if the iron-regulated expression of *IMA1/FEP3* and its differential expression in iron-deficient wild type and *clf* shoots could be explained by H3K27me3 enrichment, we performed

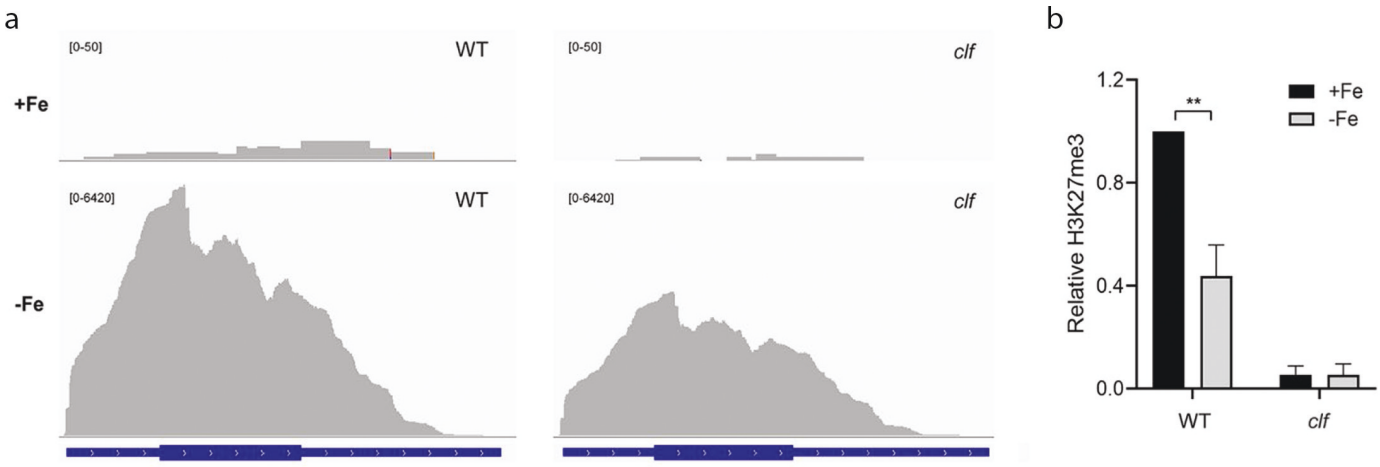

Figure 5. *IMA1* transcript level and H3K27me3 deposition in wild type and *clf* shoots. (a) RNA-seq read count histograms of *IMA1* in wild type and *clf* shoots under iron deficient and sufficient conditions. Gene diagrams depict introns (line) and exons (boxes) and are aligned with read counts. The read count range is denoted in the upper left corner of each diagram. Read count scale is equivalent for wild type and *clf* within each gene. (b) H3K27me3 deposition at *IMA1* locus. ChIP-qPCR signal was normalized with input DNA, and H3K27me3 enrichment relative to that of wild type grown under iron-sufficient conditions was plotted. Error bars represent standard error of the mean of four biological replicates and significant differences compared to wild type based on t-tests are denoted (n = 4; *: $p < .05$).

ChIP-qPCR to quantify H3K27me3 deposition in wild type and *clf* shoots treated under iron deficient and sufficient conditions. The amount of H3K27me3 deposition inversely correlated with *IMA1* transcript levels under different iron conditions in wild type (Figure 5), which suggests that the *IMA1* locus is a direct target of H3K27me3 and indicates that H3K27me3 contributes to iron-dependent regulation of *IMA1* in wild type. However, *IMA1* expression was significantly lower in iron-deficient *clf* shoots than in wild type (Figure 5(a)), despite the drastically reduced level of H3K27me3 deposition in *clf* regardless of the iron conditions (Figure 5(b)). Based on the role of *IMA1* as a regulator of the iron-deficiency response[45,46] and the enhanced iron levels in *clf* shoots (Figure 2(c)), we speculate that the reduced *IMA1* transcript levels in iron-deficient *clf* shoots are most likely the effect of enhanced iron uptake and increased level of iron in iron-deficient *clf* plants. Although *IMA1* mRNA levels were extremely low in iron-sufficient conditions, we detected a notable difference in *IMA1* transcript levels in iron-sufficient wild type and *clf* shoots (Figure 5(a)), which contain similar levels of iron (Figure 2c). Based on these results, we postulate that H3K27me3 deposition at the *IMA1* locus may play a limited role compared to the regulation by iron levels.

Discussion

Accumulating evidence suggests that regulation in response to iron availability occurs over multiple stages of gene expression, in addition to that at the transcriptional level. However, the effect of chromatin remodeling on iron homeostasis is not well understood. Compared to roots, significantly fewer studies have investigated the response to iron deficiency in shoot tissues. In this study, we extend our previous research, which focused on H3K27me3-mediated regulation of iron-acquisition genes in the roots,[47] by providing evidence that H3K27me3 mediates iron homeostasis in shoot tissues. We show that *YSL1* and *IMA1*, which play critical roles in signaling iron status from the shoots,[42,45,46] are direct targets of H3K27me3 (Figures 4 and 5). Furthermore, we report the transcriptional changes and increased iron translocation in *clf* shoots that were observed under iron-deficiency treatment. To our knowledge, the effect of H3K27me3 on iron homeostasis in shoots has not been previously reported.

Under prolonged iron deficiency, the iron content of *clf* roots and shoots is higher compared to wild type (Figure 1), as expected from the transcriptional response in roots and growth phenotype of *clf* in low iron.[47] However, after a 3-d treatment under iron deficiency, *clf* plants enhance iron translocation to the shoots rather than accumulating iron in the roots (Figure 2(d)). Considering that YSL1 functions as a transporter to load iron-NA to the leaves,[82] the higher induction of *YSL1* under iron-deficiency in *clf* shoots as compared to wild type (Figure 4(a)) agrees with the evidence of increased in iron translocation to the shoots of *clf* (Figure 2(d)). Furthermore, the inverse correlation between H3K27me3 deposition on the *YSL1* locus and iron-dependent *YSL1* expression levels in wild type and *clf* indicates the direct involvement of H3K27me3 in iron-dependent regulation of *YSL1* (Figure 4). With respect to the role of YSL1 in signaling iron status from shoots to roots,[42] the higher induction of *YSL1* in iron-deficient *clf* shoots might imply the generation of a stronger mobile signal from shoots that triggers iron uptake in response to iron deficiency. We speculate that stronger YSL1-mediated iron signaling in iron-deficient *clf* than in iron-deficient wild type may have contributed to the more robust induction of FIT-dependent iron-acquisition genes in *clf*, in addition to the effect of the reduced H3K27me3 deposition in the mutant, as detected in our previous study.[47]

Another major regulator of iron translocation is OPT3. Iron loading to the phloem by OPT3 is necessary for iron signaling from shoots to roots to regulate iron-deficiency response, and *opt3* mutants constitutively express *IRT1* and *FRO2* due to decreased iron in the phloem.[31,89] We observed differential expression of *OPT3* in *clf* and wild type after iron-deficiency treatment; the fold change induction of *OPT3* was lower in *clf* than in wild type for both roots[47] and shoots Table 1). We postulate that increased iron influx in *clf* under iron deficiency might have influenced the reduced induction of *OPT3*.

Table 2. Shoot iron homeostasis genes identified as H3K27me3 targets from existing epigenomic profiling datasets.

Gene ID	Gene Name	Annotated Function
At1g21140	*Vacuolar Iron Transporter-Like 1 (VTL1)*	iron transport into the vacuole
At1g47395	*Fe-Uptake Inducing Peptide 2/Ironman 2 (FEP2/IMA2)*	regulator of the iron deficiency response
At1g47400	*Fe-Uptake Inducing Peptide 3/Ironman 1 (FEP3/IMA1)*	regulator of the iron deficiency response
At1g65730	*Yellow Stripe Like 7 (YSL7)*	iron-nicotianamine transmembrane transporter
At1g76800	*Vacuolar Iron Transporter-Like 2 (VTL2)*	Iron transport into the vacuole
At2g30766	*Fe-Uptake Inducing Peptide 1/Ironman 3 (FEP1/IMA3)*	regulator of the iron deficiency response
At3g25190	*Vacuolar Iron Transporter-Like 5 (VTL5)*	iron transport into the vacuole
At4g24120	*Yellow Stripe Like 1 (YSL1)*	iron-nicotianamine transmembrane transporter
At4g25100	*Fe-Superoxide Dismutase 1 (FSD1)*	dismutates superoxide during oxidative stress
At5g04950	*Nicotianamine Synthase 1 (NAS1)*	synthesizes nicotianamine
At5g51720	*NEET*	2Fe-2 S cluster binding

Whether the observed differences in *OPT3* or *YSL1* transcript levels leads to differences in xylem or phloem iron levels of *clf* and wild type plants remains to be understood.

Based on our transcriptomic analysis, the profile of iron-regulated genes that were differentially expressed in *clf* shoots revealed two modes of response. First, iron-deficient *clf* shoots are undergoing transcriptional changes to buffer iron-overload and mitigate iron-induced oxidative stress. This idea is represented by the decreased repression, i.e. higher transcript levels, of *VTL*s, ROS scavenger genes, and ferritin genes (Figure 3), which are induced by iron supply or oxidative stress.[79,90] Whether the higher expression of these genes is a direct effect of chromatin remodeling due to decreased H3K27me3 in iron-deficient *clf* shoots remains to be determined. *VTL1/2/5* loci have been identified as H3K27me3 targets from epigenomic profiling studies, but *FER1/4* were not detected among the target loci (Table 2).[8,85-88,91] *FER1* is transcriptionally induced by the presence of iron,[92] but its mRNA is also subjected to iron or oxidative stress-induced degradation.[93] Thus, post-transcriptional regulation might have contributed to the difference in *FER1* transcription levels between iron-deficient *clf* and wild type shoots (Figure 3). We also note that in a recent study conducted with whole seedlings, it was shown that *FER1/3/4* were not subjected to H3K27me3 mark deposition under control conditions.[94] In contrast, histone marks that positively regulate gene expression, H3K4me3 and H3K9ac were present on the *FER1/3/4* loci.

Second, the transcriptional profile indicated that *clf* shoots were sensing less iron deficiency than wild type after iron-deficiency treatment (Figure 3). In *clf* shoots, multiple known iron-deficiency response genes, including *bHLH38/39/100/101*, *BTS*, *PYE*, and PYE-target genes, are not as strongly induced as in wild type (Figure 3). However, we note that the induction level of these genes was similar between *clf* and wild type in roots.[47] This discrepancy between the relative fold changes in the roots and shoots of wild type and *clf* indicates that the decreased induction of iron-deficiency response genes in the shoots of iron-deficient *clf* is most likely a response to a higher level of iron in their shoots, rather than a direct effect of H3K27me3. Decreased content of chlorophyll and other light-harvesting pigments is one of the main consequences of iron deficiency on photosynthesis.[95-97] Thus, the reduced repression of genes involved in photosynthesis and tetrapyrrole biosynthesis is likely due to the less severe iron deficiency perceived in *clf* leaves, as a result of more iron translocation to the shoots compared to wild type. In addition, the lower level of *IMA1* transcripts in *clf* compared to wild type implies that *clf* shoots

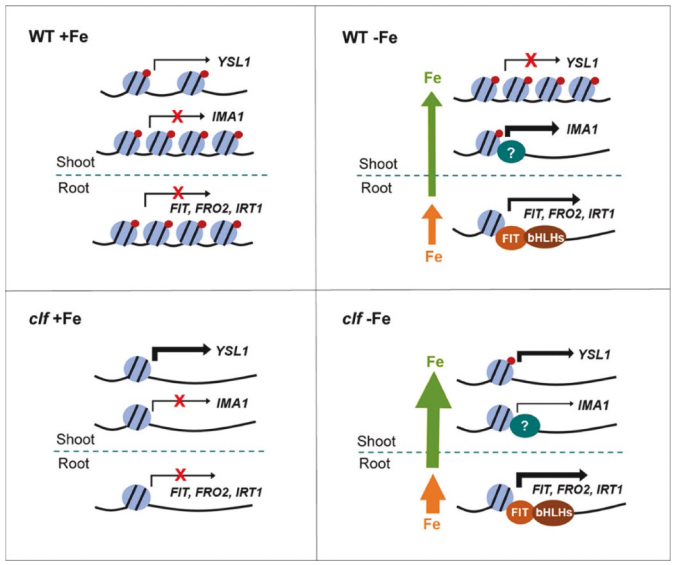

Figure 6. Proposed model for H3K27me3-mediated regulation under iron deficiency. **Upper left**: Wild type under iron-sufficient conditions (WT +Fe). H3K27me3 accumulates on FIT-dependent iron-acquisition gene loci and prevents their expression in the roots. In the shoots, moderate H3K27me3 deposition on *YSL1* locus in wild type allows for moderate *YSL1* expression, and the high H3K27me3 deposition on *IMA1* locus mediates repression. **Upper right**: Wild type under iron-deficient conditions (WT – Fe). Partial removal of H3K27me3 from FIT-dependent acquisition loci allows the induction of these genes. In the shoots, the high H3K27me3 deposition on *YSL1* locus prevents its expression. The decreased H3K27me3 deposition on the *IMA1* locus facilitates an increase in expression, but iron-responsive transcriptional regulator(s) are necessary to fully induce *IMA1*. Compared to iron-deficient *clf* plants, less high-affinity iron uptake from the soil (orange arrow) and iron translocation from roots to shoots (green arrow) occur in iron-deficient wild type. **Lower left**: Iron-sufficient *clf* mutant (*clf* +Fe). The lack of H3K27me3 in *clf* is not sufficient to induce FIT-dependent genes due to the presence of iron that negatively regulates their expression in the roots. In the shoots, the low H3K27me3 deposition on *YSL1* locus in *clf* mutants allows for higher expression of *YSL1* than in wild type from the same iron conditions. **Lower right**: Iron-deficient *clf* mutant (*clf* -Fe). Induction of iron-acquisition genes is more robust in *clf* roots, which exhibits significantly less H3K27me3 deposition on these loci. In the shoots, the low H3K27me3 deposition on *YSL1* locus in *clf* mutants allows for higher expression of *YSL1* than in wild type from the same iron conditions. Decreased H3K27me3 deposition on *IMA1* leads to an increase in expression that is dampened by higher shoot iron content compared to wild type. Compared to iron-deficient wild type, more high-affinity iron uptake from the soil (orange arrow) and iron translocation from roots to shoots (green arrow) occur in iron-deficient *clf*. Blue circles with black lines represent nucleosomes, with core histones and chromatin DNA, red circles represent H3K27me3 deposition, and the distance between blue circles depicts euchromatin or heterochromatin structure due to H3K27me3. Green circles with the question mark represent iron-responsive transcriptional regulator(s) necessary to fully induce *IMA1*, possibly bHLH121/URI and ILR3. Black arrows and their thickness represent the strength of transcriptional activity. High-affinity iron uptake under iron-deficient conditions is shown as orange arrows, and iron translocation from roots to shoots under iron-deficient conditions is indicated in green arrows. Thicker arrows represent enhanced high-affinity iron uptake from the soil or increased translocation of iron.

sense less iron deficiency than wild type (Figure 5). We detected iron-dependent H3K27me3 deposition on *IMA1* locus in wild type shoots (Figure 5), which strongly suggests that PRC2-mediated H3K27me3 controls the expression of *IMA1* under iron deficiency. However, the undetectable level of *IMA1* transcripts in iron-sufficient *clf* shoots indicates that the extremely low level of H3K27me3 is not sufficient to induce *IMA1* expression (Figure 5). We postulate that iron-responsive transcriptional regulator(s) are necessary to fully induce *IMA1* under iron-deficient conditions, and it is most likely that the higher level of iron in iron-deficient *clf* shoots limits *IMA1* transcript levels. We further speculate that the bHLH121/URI and ILR3 complex may be responsible for the difference in *IMA1* levels in iron-deficient wild type and *clf*, because *bHLH121/URI* and *ILR3* are ubiquitously expressed[22,23,98] and bHLH121/ILR3 directly activates *IMA1* under iron deficiency.[23] Meanwhile, neither bHLH121 nor ILR3 have been identified as H3K27me3 targets from epigenomic profiling datasets (Table 2),[8,85-88,91] which indicates that these transcription factors are largely H3K27me3 independent.

Overall, the results from this study and our prior report show that PRC2-mediated H3K27me3 plays a critical role in iron homeostasis (Figure 6). The significantly reduced level of H3K27me3 deposition in *clf* plants results in hyper-induction of iron-acquisition genes in the roots and more translocation of iron to the shoots. *YSL1* and *IMA1*, which are both implicated in signaling iron status from the shoots, are direct targets of H3K27me3. However, while iron-dependent regulation of *YSL1* can be explained by H3K27me3 levels, H3K27me3 appears to play a partial or indirect role in *IMA1* induction under iron deficiency. Whether increased iron translocation in *clf* compared to wild type is an effect of H3K27me3 activity or a response to higher iron influx in *clf* roots remains to be elucidated. Further studies are also needed to better understand the molecular mechanisms of iron regulation mediated by chromatin remodeling in plants.

Acknowledgments

We thank Avery Tucker, Daniel Chung, Leah Kim, and Angie Kim for technical assistance at different stages of this project.

Author contributions

JJ conceived the idea and supervised the project. EYP, KT, and EMP conducted ChIP-qPCR and prepared samples for ICP-MS. EYP prepared samples for RNA-seq and analyzed data. JJ primarily wrote the manuscript with contributions of EYP, KT, EMP. All authors have reviewed and approved the manuscript.

Disclosure statement

The authors declare that the research was conducted in the absence of any commercial or financial relationships that could be construed as a potential conflict of interest.

Funding

This work was supported by the Gregory S. Call Undergraduate Research Program to EYP and EMP, Doelling Undergraduate Research Fund to EMP, and the H. Axel Schupf '57 Fund for Intellectual Life and the National Science Foundation grant [IOS-1754969] to JJ.

ORCID

Emily Y. Park http://orcid.org/0000-0002-5696-5034
Elizabeth M. Parsons http://orcid.org/0000-0002-5962-3283
Jeeyon Jeong http://orcid.org/0000-0002-5826-2682

Data availability statement

The RNA-seq data discussed in this publication have been deposited in NCBI's Gene Expression 783 Omnibus,[99] shoot, homeostasis and are accessible through GEO Series accession number GSE149816. https://www.ncbi.nlm.nih.gov/geo/query/acc.cgi?acc=GSE149816.

References

1. Schwarz B, Bauer P. FIT, a regulatory hub for iron deficiency and stress signaling in roots, and FIT-dependent and -independent gene signatures. J. Exp. Bot. 2020;71(5):1694–1705. doi:10.1093/jxb/eraa012.
2. Kobayashi T. Understanding the complexity of iron sensing and signaling cascades in plants. Plant Cell Physiol. 2019;60:1440–1446. doi:10.1093/pcp/pcz038.
3. Gao F, Robe K, Gaymard F, Izquierdo E, Dubos C. The transcriptional control of iron homeostasis in plants: a tale of bHLH transcription factors? Front Plant Sci. 2019;10:6. doi:10.3389/fpls.2019.00006.
4. Cointry V, Vert G. The bifunctional transporter-receptor IRT 1 at the heart of metal sensing and signalling. New Phytol. 2019;223(3):1173–1178. doi:10.1111/nph.15826.
5. Colangelo EP, Guerinot ML. The essential basic helix-loop-helix protein FIT1 is required for the iron deficiency response. Plant Cell. 2004;16:3400–3412. doi:10.1105/tpc.104.024315.
6. Jakoby M, Wang H-Y, Reidt W, Weisshaar B, Bauer P. FRU (BHLH029) is required for induction of iron mobilization genes in Arabidopsis thaliana. FEBS Lett. 2004;577:528–534. doi:10.1016/j.febslet.2004.10.062.
7. Yuan YX, Zhang J, Wang DW, Ling HQ. AtbHLH29 of Arabidopsis thaliana is a functional ortholog of tomato FER involved in controlling iron acquisition in strategy I plants. Cell Res. 2005;15:613–621. doi:10.1038/sj.cr.7290331.
8. Yuan Y, Wu H, Wang N, Li J, Zhao W, Du J, Wang D, Ling H-Q. FIT interacts with AtbHLH38 and AtbHLH39 in regulating iron uptake gene expression for iron homeostasis in Arabidopsis. Cell Res. 2008;18(3):385–397. doi:10.1038/cr.2008.26.
9. Wang N, Cui Y, Liu Y, Fan H, Du J, Huang Z, Yuan Y, Wu H, Ling H-Q. Requirement and functional redundancy of Ib subgroup bHLH proteins for iron deficiency responses and uptake in. Arabidopsis Thaliana Mol Plant. 2013;6:503–513.
10. Santi S, Schmidt W. Dissecting iron deficiency-induced proton extrusion in Arabidopsis roots. New Phytol. 2009;183:1072–1084. doi:10.1111/j.1469-8137.2009.02908.x.
11. Fourcroy P, Sisó-Terraza P, Sudre D, Savirón M, Reyt G, Gaymard F, Abadía A, Abadia J, Álvarez-Fernández A, Briat J-F, *et al.* Involvement of the ABCG37 transporter in secretion of scopoletin and derivatives by Arabidopsis roots in response to iron deficiency. New Phytol. 2014;201(1):155–167. doi:10.1111/nph.12471.
12. Clemens S, Weber M. The essential role of coumarin secretion for Fe acquisition from alkaline soil. Plant Signal Behav. 2016;11:e1114197. doi:10.1080/15592324.2015.1114197.
13. Robinson NJ, Procter CM, Connolly EL, Guerinot ML. A ferric-chelate reductase for iron uptake from soils. Nature. 1999;397:694–697. doi:10.1038/17800.
14. Eide D, Broderius M, Fett J, Guerinot ML. A novel iron-regulated metal transporter from plants identified by functional expression in yeast. Proc Natl Acad Sci USA. 1996;93:5624–5628. doi:10.1073/pnas.93.11.5624.

15. Connolly EL, Fett JP, Guerinot ML. Expression of the IRT1 metal transporter is controlled by metals at the levels of transcript and protein accumulation. Plant Cell. 2002;14:1347–1357. doi:10.1105/tpc.001263.
16. Vert G, Grotz N, Dédaldéchamp F, Gaymard F, Guerinot ML, Briat J-F, Curie C. IRT1, an Arabidopsis transporter essential for iron uptake from the soil and for plant growth. Plant Cell. 2002;14(6):1223–1233. doi:10.1105/tpc.001388.
17. Varotto C, Maiwald D, Pesaresi P, Jahns P, Salamini F, Leister D. The metal ion transporter IRT1 is necessary for iron homeostasis and efficient photosynthesis in Arabidopsis thaliana. Plant J. 2002;31(5):589–599. doi:10.1046/j.1365-313X.2002.01381.x.
18. Dubeaux G, Neveu J, Zelazny E, Vert G. Metal sensing by the IRT1 transporter-receptor orchestrates its own degradation and plant Metal nutrition. Mol Cell. 2018;69:953–964.e5. doi:10.1016/j.molcel.2018.02.009.
19. Sivitz A, Grinvalds C, Barberon M, Curie C, Vert G. Proteasome-mediated turnover of the transcriptional activator FIT is required for plant iron-deficiency responses. Plant J. 2011;66:1044–1052. doi:10.1111/j.1365-313X.2011.04565.x.
20. Gratz R, Manishankar P, Ivanov R, Köster P, Mohr I, Trofimov K, Steinhorst L, Meiser J, Mai H-J, Drerup M, *et al.* CIPK11-dependent phosphorylation modulates FIT activity to promote Arabidopsis iron acquisition in response to calcium signaling. Dev Cell. 2019;48:726–740.e10. doi:10.1016/j.devcel.2019.01.006.
21. Meiser J, Lingam S, Bauer P. Posttranslational regulation of the iron deficiency basic helix-loop-helix transcription factor FIT is affected by iron and nitric oxide. Plant Physiol. 2011;157:2154–2166. doi:10.1104/pp.111.183285.
22. Kim SA, LaCroix IS, Gerber SA, Guerinot ML. The iron deficiency response in Arabidopsis thaliana requires the phosphorylated transcription factor URI. Proc Natl Acad Sci USA. 2019;116:24933–24942. doi:10.1073/pnas.1916892116.
23. Gao F, Robe K, Bettembourg M, Navarro N, Rofidal V, Santoni V, Gaymard F, Vignols F, Roschzttardtz H, Izquierdo E, *et al.* The transcription factor bHLH121 interacts with bHLH105 (ILR3) and its closest homologs to regulate iron homeostasis in Arabidopsis. Plant Cell. 2020;32:508–524. doi:10.1105/tpc.19.00541.
24. Long TA, Tsukagoshi H, Busch W, Lahner B, Salt DE, Benfey PN. The bHLH transcription factor POPEYE regulates response to iron deficiency in Arabidopsis roots. Plant Cell. 2010;22:2219–2236. doi:10.1105/tpc.110.074096.
25. Bauer P, Thiel T, Klatte M, Bereczky Z, Brumbarova T, Hell R, Grosse I. Analysis of sequence, map position, and gene expression reveals conserved essential genes for iron uptake in Arabidopsis and tomato. Plant Physiol. 2004;136(4):4169–4183. doi:10.1104/pp.104.047233.
26. Jeong J, Connolly EL. Iron uptake mechanisms in plants: functions of the FRO family of ferric reductases. Plant Sci. 2009;176:709–714. doi:10.1016/j.plantsci.2009.02.011.
27. Selote D, Samira R, Matthiadis A, Gillikin JW, Long TA. Iron-binding E3 ligase mediates iron response in plants by targeting basic helix-loop-helix transcription factors. Plant Physiol. 2015;167:273–286. doi:10.1104/pp.114.250837.
28. Hindt MN, Akmakjian GZ, Pivarski KL, Punshon T, Baxter I, Salt DE, Guerinot ML. BRUTUS and its paralogs, BTS LIKE1 and BTS LIKE2, encode important negative regulators of the iron deficiency response in Arabidopsis thaliana. Metallomics. 2017;9(7):876–890. doi:10.1039/C7MT00152E.
29. Morrissey J, Baxter IR, Lee J, Li L, Lahner B, Grotz N, Kaplan J, Salt DE, Guerinot ML. The ferroportin metal efflux proteins function in iron and cobalt homeostasis in Arabidopsis. Plant Cell. 2009;21:3326–3338. doi:10.1105/tpc.109.069401.
30. Durrett TP, Gassmann W, Rogers EE. The FRD3-mediated efflux of citrate into the root vasculature is necessary for efficient iron translocation. Plant Physiol. 2007;144:197–205. doi:10.1104/pp.107.097162.
31. Zhai Z, Gayomba SR, Jung H-I, Vimalakumari NK, Piñeros M, Craft E, Rutzke MA, Danku J, Lahner B, Punshon T, et al. OPT3 is a phloem-specific iron transporter that is essential for systemic iron signaling and redistribution of iron and cadmium in Arabidopsis. Plant Cell. 2014;26(5):2249–2264. doi:10.1105/tpc.114.123737.
32. von Wiren N, Klair S, Bansal S, Briat J-F, Khodr H, Shioiri T, Leigh RA, Hider RC. Nicotianamine chelates both Fe III and Fe II implications for metal transport in plants. Plant Physiol. 1999;119:1107–1114. doi:10.1104/pp.119.3.1107.
33. DiDonato RJ, Roberts LA, Sanderson T, Eisley RB, Walker EL. Arabidopsis Yellow Stripe-Like2 (YSL2): a metal-regulated gene encoding a plasma membrane transporter of nicotianamine-metal complexes. Plant J. 2004;39:403–414. doi:10.1111/j.1365-313X.2004.02128.x.
34. Schaaf G, Schikora A, Häberle J, Vert G, Ludewig U, Briat J-F, Curie C, von Wirén N. A putative function for the arabidopsis Fe-Phytosiderophore transporter homolog AtYSL2 in Fe and Zn homeostasis. Plant Cell Physiol. 2005;46:762–774. doi:10.1093/pcp/pci081.
35. Chu -H-H, Chiecko J, Punshon T, Lanzirotti A, Lahner B, Salt DE, Walker EL. Successful reproduction requires the function of arabidopsis yellow stripe-like1 and yellow stripe-like3 metal-nicotianamine transporters in both vegetative and reproductive structures. Plant Physiol. 2010;154(1):197–210. doi:10.1104/pp.110.159103.
36. Maas FM, van de Wetering DA, van Beusichem ML, Bienfait HF. Characterization of phloem iron and its possible role in the regulation of fe-efficiency reactions. Plant Physiol. 1988;87:167–171. doi:10.1104/pp.87.1.167.
37. Grusak MA, Pezeshgi S. Shoot-to-root signal transmission regulates root Fe(III) reductase activity in the dgl mutant of pea. Plant Physiol. 1996;110:329–334. doi:10.1104/pp.110.1.329.
38. Romera FJ, Alcántara E, de la Guardia MD. Role of roots and shoots in the regulation of the Fe efficiency responses in sunflower and cucumber. Physiol Plant. 1992;85:141–146. doi:10.1111/j.1399-3054.1992.tb04716.x.
39. Enomoto Y, Hodoshima H, Shimada H, Shoji K, Yoshihara T, Goto F. Long-distance signals positively regulate the expression of iron uptake genes in tobacco roots. Planta. 2007;227:81–89. doi:10.1007/s00425-007-0596-x.
40. Vert GA, Briat J-F, Curie C. Dual regulation of the Arabidopsis high-affinity root iron uptake system by local and long-distance signals. Plant Physiol. 2003;132:796–804. doi:10.1104/pp.102.016089.
41. García MJ, Romera FJ, Stacey MG, Stacey G, Villar E, Alcántara E, Pérez-Vicente R. Shoot to root communication is necessary to control the expression of iron-acquisition genes in strategy I plants. Planta. 2013;237(1):65–75. doi:10.1007/s00425-012-1757-0.
42. Kumar RK, Chu -H-H, Abundis C, Vasques K, Rodriguez DC, Chia J-C, Huang R, Vatamaniuk OK, Walker EL. Iron-nicotianamine transporters are required for proper long distance iron signaling. Plant Physiol. 2017;175(3):1254–1268. doi:10.1104/pp.17.00821.
43. Rogers EE, Guerinot ML. FRD3, a member of the multidrug and toxin efflux family, controls iron deficiency responses in Arabidopsis. Plant Cell. 2002;14:1787–1799. doi:10.1105/tpc.001495.
44. Klatte M, Schuler M, Wirtz M, Fink-Straube C, Hell R, Bauer P. The analysis of Arabidopsis nicotianamine synthase mutants reveals functions for nicotianamine in seed iron loading and iron deficiency responses. Plant Physiol. 2009;150:257–271. doi:10.1104/pp.109.136374.
45. Grillet L, Lan P, Li W, Mokkapati G, Schmidt W. IRON MAN is a ubiquitous family of peptides that control iron transport in plants. Nat Plants. 2018;4:953–963. doi:10.1038/s41477-018-0266-y.
46. Hirayama T, Lei GJ, Yamaji N, Nakagawa N, Ma JF. The putative peptide gene FEP1 regulates iron deficiency response in arabidopsis. Plant Cell Physiol. 2018;59:1739–1752. doi:10.1093/pcp/pcy145.
47. Park EY, Tsuyuki KM, Hu F, Lee J, Jeong J. PRC2-mediated H3K27me3 contributes to transcriptional regulation of FIT-dependent iron deficiency response. Front Plant Sci. 2019;10:627. doi:10.3389/fpls.2019.00627.

48. Köhler C, Hennig L. Regulation of cell identity by plant polycomb and trithorax group proteins. Curr Opin Genet Dev. 2010;20:541–547. doi:10.1016/j.gde.2010.04.015.
49. Pu L, Sung ZR. PcG and trxG in plants – friends or foes. Trends Genet. 2015;31:252–262. doi:10.1016/j.tig.2015.03.004.
50. Chanvivattana Y, Bishopp A, Schubert D, Stock C, Moon YH, Sung ZR, Goodrich J. Interaction of Polycomb-group proteins controlling flowering in Arabidopsis. Development. 2004;131:5263–5276. doi:10.1242/dev.01400.
51. Wang H, Liu C, Cheng J, Liu J, Zhang L, He C, Shen W-H, Jin H, Xu L, Zhang Y, *et al*. Arabidopsis flower and embryo developmental genes are repressed in seedlings by different combinations of polycomb group proteins in association with distinct sets of cis-regulatory elements. PLoS Genet. 2016;12(1):e1005771. doi:10.1371/journal.pgen.1005771.
52. Deng W, Buzas DM, Ying H, Robertson M, Taylor J, Peacock W, Dennis ES, Helliwell C. Arabidopsis polycomb repressive complex 2 binding sites contain putative GAGA factor binding motifs within coding regions of genes. BMC Genomics. 2013;14(1):593. doi:10.1186/1471-2164-14-593.
53. Margueron R, Reinberg D. The polycomb complex PRC2 and its mark in life. Nature. 2011;469:343–349. doi:10.1038/nature09784.
54. Gamborg OL, Miller RA, Ojima K. Nutrient requirements of suspension cultures of soybean root cells. Exp Cell Res. 1968;50:151–158. doi:10.1016/0014-4827(68)90403-5.
55. Murashige T, Skoog F. A revised medium for rapid growth and bio assays with tobacco tissue cultures. Physiol Plant. 1962;15:473–497. doi:10.1111/j.1399-3054.1962.tb08052.x.
56. Aranda PS, LaJoie DM, Jorcyk CL. Bleach gel: a simple agarose gel for analyzing RNA quality. Electrophoresis. 2012;33:366–369. doi:10.1002/elps.201100335.
57. Robinson JT, Thorvaldsdóttir H, Winckler W, Guttman M, Lander ES, Getz G, Mesirov JP. Integrative genomics viewer. Nat Biotechnol. 2011;29:24–26. doi:10.1038/nbt.1754.
58. Thorvaldsdóttir H, Robinson JT, Mesirov JP. Integrative Genomics Viewer (IGV): high-performance genomics data visualization and exploration. Brief Bioinform. 2013;14:178–192. doi:10.1093/bib/bbs017.
59. Anders S, Huber W. Differential expression analysis for sequence count data. Genome Biol. 2010;11:R106. doi:10.1186/gb-2010-11-10-r106.
60. Mi H, Huang X, Muruganujan A, Tang H, Mills C, Kang D, Thomas PD. PANTHER version 11: expanded annotation data from gene ontology and reactome pathways, and data analysis tool enhancements. Nucleic Acids Res. 2017;45:D183–D189. doi:10.1093/nar/gkw1138.
61. Ashburner M, Ball CA, Blake JA, Bolstein D, Butler H, Cherry JM, Davis AP, Dolinski K, Dwight SS, Eppig JT, et al. Gene Ontology: tool for the unification of biology. Nat Genet. 2000;25:25–29. doi:10.1038/75556.
62. *The Gene Ontology Consortium*. Expansion of the Gene Ontology knowledgebase and resources. Nucleic Acids Res. 2017;45:D331–D338. doi:10.1093/nar/gkw1108.
63. Haring M, Offermann S, Danker T, Horst I, Peterhansel C, Stam M. Chromatin immunoprecipitation: optimization, quantitative analysis and data normalization. Plant Methods. 2007;3:11. doi:10.1186/1746-4811-3-11.
64. Arvidsson S, Kwasniewski M, Riaño-Pachón DM, Mueller-Roeber B. QuantPrime–a flexible tool for reliable high-throughput primer design for quantitative PCR. BMC Bioinformatics. 2008;9:465. doi:10.1186/1471-2105-9-465.
65. Xu L, Shen W-H. Polycomb silencing of KNOX genes confines shoot stem cell niches in Arabidopsis. Curr Biol. 2008;18:1966–1971. doi:10.1016/j.cub.2008.11.019.
66. Schönrock N, Bouveret R, Leroy O, Borghi L, Kohler C, Gruissem W, Hennig L. Polycomb-group proteins repress the floral activator AGL19 in the FLC-independent vernalization pathway. Genes Dev. 2006;20:1667–1678. doi:10.1101/gad.377206.
67. Bouveret R, Schönrock N, Gruissem W, Hennig L. Regulation of flowering time by Arabidopsis MSI1. Development. 2006;133:1693–1702. doi:10.1242/dev.02340.
68. de Lucas M, Pu L, Turco G, Gaudinier A, Morao AK, Kim D, Ron M, Sugimoto K, Roudier F, Brady SM. Transcriptional regulation of Arabidopsis polycomb repressive complex 2 coordinates cell-type proliferation and differentiation. Plant Cell. 2016;28(10):2616–2631. doi:10.1105/tpc.15.00744.
69. Zhao W, Shafiq S, Berr A, Shen W-H. Genome-wide gene expression profiling to investigate molecular phenotypes of Arabidopsis mutants deprived in distinct histone methyltransferases and demethylases. Genom Data. 2015;4:143–145. doi:10.1016/j.gdata.2015.04.006.
70. Bellegarde F, Herbert L, Séré D, Caillieux E, Boucherez J, Fizames C, Roudier F, Gojon A, Martin A. Polycomb Repressive Complex 2 attenuates the very high expression of the Arabidopsis gene NRT2.1. Sci Rep. 2018;8:7905. doi:10.1038/s41598-018-26349-w.
71. Halkier BA, Gershenzon J. Biology and biochemistry of glucosinolates. Annu Rev Plant Biol. 2006;57:303–333. doi:10.1146/annurev.arplant.57.032905.105228.
72. Backenköhler A, Eisenschmidt D, Schneegans N, Strieker M, Brandt W, Wittstock U. Iron is a centrally bound cofactor of specifier proteins involved in glucosinolate breakdown. PLoS One. 2018;13(11):e0205755. doi:10.1371/journal.pone.0205755.
73. Pan I-C, Tsai HH, Chengy YT, Wen TN, Buckhout TJ, Schmidt W. Post-transcriptional coordination of the arabidopsis iron deficiency response is partially dependent on the E3 ligases RING DOMAIN LIGASE1 (RGLG1) and RING DOMAIN LIGASE2 (RGLG2). Mol Cell Proteomics. 2015;14:2733–2752. doi:10.1074/mcp.M115.048520.
74. Jeong J, Cohu C, Kerkeb L, Pilon M, Connolly EL, Guerinot ML. Chloroplast Fe(III) chelate reductase activity is essential for seedling viability under iron limiting conditions. Proc Natl Acad Sci USA. 2008;105:10619–10624. doi:10.1073/pnas.0708367105.
75. Zimmermann P, Hirsch-Hoffmann M, Hennig L, Gruissem W. GENEVESTIGATOR. Arabidopsis microarray database and analysis toolbox. Plant Physiol. 2004;136:2621–2632. doi:10.1104/pp.104.046367.
76. Higuchi K, Suzuki K, Nakanishi H, Yamaguchi H, Nishizawa N-K, Mori S. Cloning of nicotianamine synthase genes, novel genes involved in the biosynthesis of phytosiderophores. Plant Physiol. 1999;119(2):471–480. doi:10.1104/pp.119.2.471.
77. Conte SS, Walker EL. Genetic and biochemical approaches for studying the yellow stripe-like transporter family in plants. Curr Top Membr. 2012;69:295–322.
78. Ravet K, Touraine B, Boucherez J, Briat J-F, Gaymard F, Cellier F. Ferritins control interaction between iron homeostasis and oxidative stress in Arabidopsis. Plant J. 2009;57(3):400–412. doi:10.1111/j.1365-313X.2008.03698.x.
79. Gollhofer J, Timofeev R, Lan P, Schmidt W, Buckhout TJ. Vacuolar-Iron-Transporter1-Like proteins mediate iron homeostasis in Arabidopsis. PLoS One. 2014;9:e110468. doi:10.1371/journal.pone.0110468.
80. Pnueli L, Liang H, Rozenberg M, Mittler R. Growth suppression, altered stomatal responses, and augmented induction of heat shock proteins in cytosolic ascorbate peroxidase (Apx1)-deficient Arabidopsis plants. Plant J. 2003;34:187–203. doi:10.1046/j.1365-313X.2003.01715.x.
81. Alscher RG, Erturk N, Heath LS. Role of superoxide dismutases (SODs) in controlling oxidative stress in plants. J Exp Bot. 2002;53:1331–1341. doi:10.1093/jexbot/53.372.1331.
82. Waters BM, Chu -H-H, DiDonato RJ, Roberts LA, Eisley RB, Lahner B, Salt DE, Walker EL. Mutations in Arabidopsis yellow stripe-like1 and yellow stripe-like3 reveal their roles in metal ion homeostasis and loading of metal ions in seeds. Plant Physiol. 2006;141(4):1446–1458. doi:10.1104/pp.106.082586.
83. Roudier F, Ahmed I, Bérard C, Sarazin A, Mary-Huard T, Cortijo S, Bouyer D, Caillieux E, Duvernois-Berthet E, Al-Shikhley L, *et al*. Integrative epigenomic mapping defines four main chromatin states in Arabidopsis. Embo J. 2011;30:1928–1938. doi:10.1038/emboj.2011.103.
84. Turck F, Roudier F, Farrona S, Martin-Magniette M-L, Guillaume E, Buisine N, Gagnot S, Martienssen RA, Coupland G, Colot V, *et al*. Arabidopsis TFL2/LHP1 specifically associates with

genes marked by trimethylation of histone H3 lysine 27. PLoS Genet. 2007;3:e86. doi:10.1371/journal.pgen.0030086.
85. Zhang X, Clarenz O, Cokus S, Bernatavichute YV, Pellegrini M, Goodrich J, Jacobsen SE. Whole-genome analysis of histone H3 lysine 27 trimethylation in Arabidopsis. PLoS Biol. 2007;5(5):e129. doi:10.1371/journal.pbio.0050129.
86. Bouyer D, Roudier F, Heese M, Andersen ED, Gey D, Nowack MK, Goodrich J, Renou J-P, Grini PE, Colot V, *et al*. Polycomb repressive complex 2 controls the embryo-to-seedling phase transition. PLoS Genet. 2011;7(3):e1002014. doi:10.1371/journal.pgen.1002014.
87. Lafos M, Kroll P, Hohenstatt ML, Thrope FL, Clarenz O, schubert D. Dynamic regulation of H3K27 trimethylation during Arabidopsis differentiation. PLoS Genet. 2011;7:e1002040. doi:10.1371/journal.pgen.1002040.
88. Lu F, Cui X, Zhang S, Jenuwein T, Cao X. Arabidopsis REF6 is a histone H3 lysine 27 demethylase. Nat Genet. 2011;43:715–719. doi:10.1038/ng.854.
89. Khan MA, Castro-Guerrero NA, McInturf SA, Nguyen NT, Dame AN, Wang J, Bindbeutel RK, Joshi T, Jurisson SS, Nusinow DA, et al. Changes in iron availability in Arabidopsis are rapidly sensed in the leaf vasculature and impaired sensing leads to opposite transcriptional programs in leaves and roots. Plant Cell Environ. 2018;41:2263–2276. doi:10.1111/pce.13192.
90. Briat J-F, Ravet K, Arnaud N, Duc C, Boucherez J, Touraine B, Cellier F, Gaymard F. New insights into ferritin synthesis and function highlight a link between iron homeostasis and oxidative stress in plants. Ann Bot. 2010;105:811–822. doi:10.1093/aob/mcp128.
91. Farrona S, Thrope FL, Engelhorn J, Adrian J, Dong X, Sarid-Krebs L, Goodrich J, Turck F. Tissue-specific expression of FLOWERING LOCUS T in Arabidopsis is maintained independently of polycomb group protein repression. Plant Cell. 2011;23:3204–3214. doi:10.1105/tpc.111.087809.
92. Petit JM, van Wuytswinkel O, Briat JF, Lobréaux S. Characterization of an iron-dependent regulatory sequence involved in the transcriptional control of AtFer1 and ZmFer1 plant ferritin genes by iron. J Biol Chem. 2001;276:5584–5590. doi:10.1074/jbc.M005903200.
93. Ravet K, Reyt G, Arnaud N, Krouk G, Djouani E-B, Boucherez J, Briat J-F, Gaymard F. Iron and ROS control of the downstream mRNA decay pathway is essential for plant fitness. Embo J. 2012;31(1):175–186. doi:10.1038/emboj.2011.341.
94. Tissot N, Robe K, Gao F, Grant-Grant S, Boucherez J, Bellegarde F, Maghiaoui A, Marcelin R, Izquierdo E, Benhamed M, et al. Transcriptional integration of the responses to iron availability in Arabidopsis by the bHLH factor ILR3. New Phytol. 2019. doi:10.1111/nph.15753.
95. Glover H. Effects of iron deficiency on isochrysis galbana (chrysophyceae) and phaeodactylum tricornutum (bacillariophyceae). J Phycol. 1977;13:208–212.
96. Greene RM, Geider RJ, Falkowski PG. Effect of iron limitation on photosynthesis in a marine diatom. Limnol Oceangr. 1991;36:1772–1782. doi:10.4319/lo.1991.36.8.1772.
97. van Leeuwe MA, Stefels J. Effects of iron and light stress on the biochemical composition of antarctic phaeocystis sp. (prymnesiophyceae). Ii. Pigment composition. J Phycol. 1998;34:496–503. doi:10.1046/j.1529-8817.1998.340496.x.
98. Rampey RA, Woodward AW, Hobbs BN, Tierney MP, Lahner B, Salt DE, Bartel B. An Arabidopsis basic helix-loop-helix leucine zipper protein modulates metal homeostasis and auxin conjugate responsiveness. Genetics. 2006;174:1841–1857. doi:10.1534/genetics.106.061044.
99. Edgar R, Domrachev M, Lash AE. Gene Expression Omnibus: NCBI gene expression and hybridization array data repository. Nucleic Acids Res. 2002;30:207–210. doi:10.1093/nar/30.1.207.